Building leakage, infiltration, and energy performance analyses for Finnish detached houses

Juha Jokisalo [a,*], Jarek Kurnitski [a], Minna Korpi [b], Targo Kalamees [a], Juha Vinha [b]

[a] HVAC-Laboratory, Helsinki University of Technology, P.O. Box 4400, FIN-02015, TKK, Finland
[b] Department of Civil Engineering, Tampere University of Technology, P.O. Box 600, 33101 Tampere, Finland

ARTICLE INFO

ABSTRACT

This study focuses on the relation between the airtightness of a building envelope, infiltration, and energy use of a typical modern Finnish detached house in the cold climate of Finland. The study is conducted with an empirically tested dynamic IDA-ICE simulation model of a detached house. The effect of several factors, such as Finnish climate and wind conditions, balance of ventilation system and leakage distribution, on infiltration was studied and a simple adapted model for the rough estimation of annual infiltration in Finnish detached houses was determined from the numerical simulation results. The energy impact of infiltration is also studied, taking into account the infiltration heat recovery effect. According to the results, infiltration causes about 15–30% of the energy use of space heating including ventilation in the typical Finnish detached house. The average infiltration rate and heat energy use increase almost linearly with the building leakage rate n_{50}. Finland can be roughly divided into two zones based on the average infiltration rate of detached houses, for which stack-induced infiltration is typically dominant, regardless of the climate zone. The infiltration heat recovery effect is minor in the studied detached house.

© 2008 Elsevier Ltd. All rights reserved.

1. Introduction

The European energy performance directive for buildings (Energy Performance Building Directive-EPBD) states that the energy efficiency of buildings has to be calculated in the member states [1]. The member states are implementing the EPBD at the national level by taking into account local climate and conditions, requirements for indoor climate and cost efficiency. An objective is that the directive will be implemented in all member states by 4th of January 2009 at the latest. Infiltration of buildings has a significant effect on the energy performance of buildings; this depends on climate conditions and factors that are related to, for example, the type of building or construction. In the updated Finnish building code [2], the average infiltration rate is calculated by dividing a single pressurization test result n_{50} by 25, where n_{50} is leakage air change rate per hour at 50 Pa of pressure difference.

Since the late 1970s, studies have been conducted on the correlation between airtightness of a building envelope and annual infiltration rate. Kronvall and Persily compared pressurization test results to infiltration rates measured with tracer-gas in detached and terraced houses in Sweden and USA (New Jersey) [3]. From their comparison, they obtained the widely used "rule of thumb" for annual infiltration rate: n_{50} divided by 20 [4]. In 1987, Sherman [4] developed a simple model, n_{50}/N, from the LBL infiltration model for the annual infiltration rate of detached houses in North America, where a correlation factor N was expressed as a product of several factors, depending on climate zone, wind shielding, height of house, and size of cracks. According to the extensive measurements that were carried out in several European countries and reported by Dubrul in 1988 [5], the denominator of the preceding relation ranges from 10 to 30, depending on, for example, the type of the building, wind conditions, and leakage distribution.

Normally, in studies related to the energy impact of infiltration, the conduction and infiltration heat losses are simply calculated on the basis of the temperature difference between inside and outside air, while the conduction and infiltration are treated as two independent processes. Since 1985, when Kohonen et al. [6] published their experimental and numerical study concerning thermal coupling of leakage air and heat flows in a building envelope, the heat recovery effect between infiltration air and exterior walls have been studied by several authors, in, for example [7–9]. This phenomenon is utilized especially with the dynamic insulation walls that are intentionally made porous, but

* Corresponding author. Tel.: +358 9 451 3598; fax: +358 9 451 3418.
E-mail address: juha.jokisalo@tkk.fi (J. Jokisalo).

Table 1
Average depressurization test results of the Finnish detached houses with different types of construction

Wall structure	Number	n_{50} (ach)		n (dimensionless)	
		Mean	Std. dev.	Mean	Std. dev.
Timber frame	100	3.9	1.8	0.72	0.06
Log	20	5.8	3.2	0.76	0.06
Autoclaved aerated concrete	10	1.5	0.6	0.72	0.04
Light expanded clay aggregate	10	3.1	1.2	0.69	0.05
Brick	10	2.7	1.2	0.74	0.06
Shuttering concrete block	10	1.6	0.8	0.76	0.06
Concrete sandwich element	10	2.6	1.1	0.73	0.04
Total (concrete/brick/lightweight block)	50	2.3	1.2	0.73	0.05
Total (all the structures)	170	3.7	2.2	0.73	0.06

the infiltration heat recovery (IHR) effect has been proven to decrease the energy use of the building, even if the infiltration air flows mainly through the cracks. Numerical and analytical models have been developed, but, until now, this phenomenon has not been taken into account in the building energy simulation software available for third parties.

The objective of this study is to find a relation between the airtightness of a building envelope, the average infiltration and energy use of a typical modern detached house in the cold climate of Finland, and to study the effect of other important factors, such as leakage distribution, wind and climate conditions, on infiltration, using the IDA-ICE simulation tool, which combines whole-building energy simulation and infiltration modelling. The purpose of the study is also to adapt a simple and usable model for the average infiltration rate of detached houses in Finnish conditions, taking all the important factors into account. Energy use of the house is simulated and the IHR effect is taken into account with an analytical model developed by Buchanan and Sherman [8].

2. Methods

This study is carried out as a sensitivity analysis simulating a single-building model under various conditions. The simulation model corresponds to an existing detached house and the applicability of this model for infiltration and energy analyses has been proved in the previous study [10]. In that study, the simulated and measured indoor air temperatures and pressure conditions of the house were compared during a 3-week test period in the heating season and the results were found to be in reasonable agreement.

2.1. Measurements

The initial data of the study concerning airtightness of Finnish detached houses were obtained with extensive field measurements from 170 detached houses [11,12]. The airtightness of these houses has been tested using a standardized fan pressurization method [13]. The measured houses were newly built detached houses with different types of construction, including variety of structures from lightweight (timber frame) to massive (concrete, brick, and lightweight block) structures. The power-law equation is fitted to pressure differences and the corresponding leakage air flows

$$Q = C \Delta P^n, \tag{1}$$

where Q is the leakage air mass flow, kg/s, C the flow coefficient that is related to the size of the opening, kg/s,Pa^n, ΔP the pressure
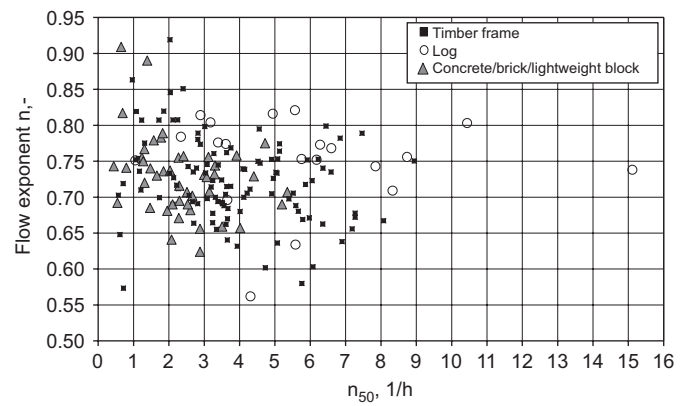

Fig. 1. The building leakage rate and the flow exponent of the studied detached houses divided into three categories according to their respective building structure.

difference across the envelope, Pa, and n the flow exponent characterizing the flow regime. The leakage openings with larger flow resistance because of longer length or narrowed widths tend to have a flow exponent that is closer to one than the openings with less flow resistance [14]. The building leakage rate n_{50} can be calculated by means of leakage air flow Q at 50 Pa pressure difference ΔP (Eq. (1)), when the internal air volume of the house is known. According to the preceding studies, the average building leakage rate n_{50} of all the studied 170 houses is 3.7 ach, see Table 1. The particular type of construction used has an effect on airtightness, because the average building leakage rate of the massive (concrete, brick, and lightweight block houses) was 2.3 ach, while the average of the timber frame and the log houses were 3.9 and 5.8 ach. According to the measurement results, the type of construction has only a minor effect on the flow exponent (see Table 1); no clear correlation between flow exponent and building leakage rate can be found with the studied buildings, see Fig. 1. The average flow exponent of all the studied houses is 0.73, being slightly higher that the mean value of 0.66 according to several studies made in five countries [15]. Over 90% of the flow exponents in this study were in the range of 0.73 ± 0.1.

A majority of the studied detached houses are timber-frame houses, as is also the case with the detached houses in the Finnish building stock. The average proportion of timber-frame detached houses of the new prefabricated detached houses has been about 80% between 1989 and 2007 in Finland, while the proportion of log and massive houses have been 12% and 8% during this period [16]. The average level of airtightness of the newly built detached

houses in Finland can be roughly estimated by weighting the average building leakage rates by the preceding proportions of the building types; the result is 4 ach.

Kalamees et al. [17] studied the distribution of the leakage openings using a two-phase thermography test of the envelope. According to the preceding air leakage distribution study of Finnish houses, typical air leakages were around and through windows and doors, at the junction of ceiling/floor with the external wall, and penetrations through the air barrier systems. A simple method to produce a resultant leakage distribution on the basis of a thermography test is shown in, for example [10].

2.2. Building description

The modelling object is a two-story detached house (see Fig. 2) corresponding to the typical detached house defined in [11]. The net floor area of the building is 172 m² and the structures of the house are timber-frame construction insulated with mineral wool and provided with a plastic air–vapor barrier. The base floor of the house is a concrete slab on the ground and the level of thermal insulation of the house ($U_{ext.wall} = 0.21$ W/m² K, $U_{roof} = 0.14$ W/m² K, $U_{basefloor} = 0.27$ W/m² K and $U_{windows} = 1.0$ W/m² K) fulfils the requirements of the Finnish building code [18]. The house is equipped with a mechanical supply and exhaust ventilation system. An original defrost protection method of ventilation heat recovery of the modelling object is based on the stopping of the supply fan, but this study uses the defrost protection method, where the supply air is bypassed with dampers. The house is heated via an electrical floor heating system and ceiling-mounted radiant panels, but the house is not equipped with mechanical cooling.

In the simulation model, the set point of heating is 21 °C and the total internal heat gains from four occupants, lighting and devices is 42 kWh/m², corresponding to the level shown in [2,19]. The schedules for the presence of the occupants and use of the lighting and devices correspond with the lifestyle of working townspeople.

Some of the rooms in the detached house were combined into one zone in the simulation model (see Fig. 3) and the rate of ventilation corresponds to 0.56 ach in all the studied cases, while the minimum requirement of the Finnish building code is 0.5 ach [20]. The supply and extraction air flow rates are shown in the case of the balanced ventilation system, see Fig. 3. The effect of the
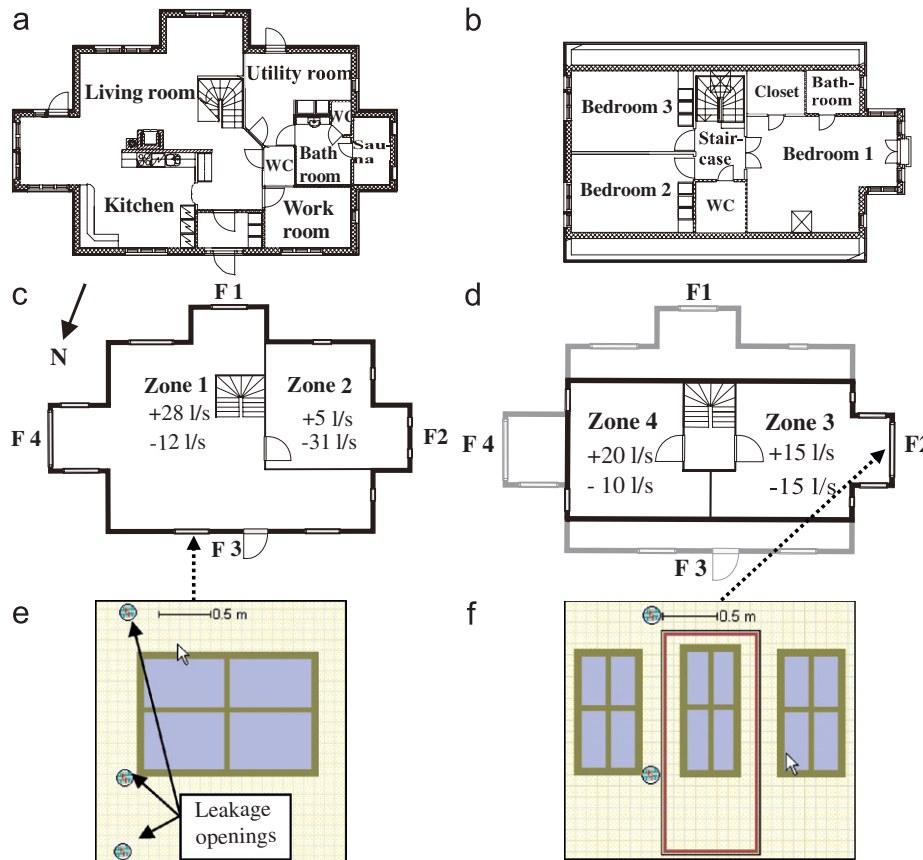

Fig. 2. The object of the study is a detached house.

Fig. 3. A plan of the base floor (a) and the top floor (b) of the simulated house, the floor plan of the simulation model (c, d) and bi-directional leakage openings situated in the wall of the model (e, f). Supply air flow rates in the balanced ventilation system are shown with a (+) sign and extract air flow rates with a (−) sign.

Table 2
The vertical leakage distributions of the house

Place of the leakage routes	Vertical leakage distribution (%)				
	Typical (two floors)	Draughty roof	Draughty base floor	Draughty roof/base floor	Typical (one floor)
Top floor					
Junction of roof	36	75	12.5	50	50
Upper edge of window frame	4	0	0	0	–
Lower edge of window frame	4	0	0	0	–
Junction of intermediate floor	2	0	0	0	–
Base floor					
Junction of intermediate floor	21	12.5	12.5	0	–
Upper edge of window	0	0	0	0	15
Lower edge of window frame	24	0	0	0	15
Junction of base floor	10	12.5	75	50	20

The typical distributions are based on the infrared photography; the three other distributions are approximated.

Table 3
Terrain parameters of the wind profile equation

Surrounding	k	a	Description
Exposed	1	0.15	Flat terrain with some isolated objects well separated from each others
Rural	0.85	0.2	Rural area with some isolated buildings or trees
Suburban	0.67	0.25	Urban, industrial or forest area

balance of the ventilation system on infiltration is studied also with supply air flow rates 15% greater or less than the extract air flow rates. But, even if the ventilation system is balanced, the differences in airflow rates for different room types induce pressure differences over the envelope, depending on the airtightness of the envelope and flow resistances between the rooms. In the simulation model, internal doors are assumed to be open on the top floor, while the door between zones (1 and 2) on the base floor is assumed to be slightly ajar (10 mm). But, the effect of internal flow resistances on the infiltration rate is also approximated by simulating the model, assuming all doors to be open or closed.

Because the height of the building has an effect on the infiltration rate, the modelling object is also simulated as a one-story house with the base floor alone. The modelling object is also simulated with different distributions of leakage openings, see Table 2. The typical leakage distribution of the two-story house shown in the table corresponds to the measured leakage distribution of the modelling object, while the typical leakage distribution of the one-story house is considered to be normal according to the measurements shown in [17]. The other leakage distributions shown by Table 2 are estimated. A total of 12–24 leakage openings were modelled, depending on the case.

2.3. Computational model

This sensitivity analysis was carried out using the simulation model of the preceding detached house. The pressure conditions of this house model were compared against measurement results [10]. The building model was formed using IDA ndoor Climate and Energy 3.0 (IDA-ICE) building simulation software. This software allows the modelling of a multi-zone building, HVAC-systems, internal and solar loads, outdoor climate, etc. and provides simultaneous dynamic simulation of heat transfer and air flows. A performance of IDA-ICE is studied in, for example [21–24].

Wind pressure distribution around the house is simulated using the normal assumption in building engineering that the wind flow is horizontal and an atmospheric boundary layer is neutral without vertical air flow. The wind pressure outside the building facades P_w is determined by

$$P_w = C_p \tfrac{1}{2} \rho_{out} U^2, \tag{2}$$

where C_p is the wind pressure coefficient, ρ_{out} the outdoor air density, kg/m^3, and U the local wind velocity, m/s, which was approximated using the wind profile equation reported in [14]. The profile that basically corresponds to the LBL model wind profile [25] is

$$U(h) = U_m k \left(\frac{h}{h_m}\right)^a, \tag{3}$$

where $U(h)$ is the wind speed at height h, m/s, U_m the wind speed measured in open country at the weather station, m/s, h the height from the surface of the ground, m, h_m the height of the measurement equipment, m, and parameters k and a the terrain-dependent constants. The wind profile equation was simulated using values for terrain parameters shown in Table 3, corresponding to the values of the different terrain classes published in [25].

The values of the wind pressure coefficients used in this study were presented in [26] (see Table 4). These wind pressure coefficients are approximated values for low-rise buildings and their applicability for the modelling object in the sheltered wind conditions was shown in [10].

The air flow through a leakage opening Q is simulated in the building model with a linearized power-law equation around a zero pressure difference resulting from numerical reasons, see Eq. (4). The normal power-law equation shown in Eq. (1), is used when the pressure difference equals or exceeds a limit value of linearization dp_0 [21]. The linearized power-law equation is defined as

$$Q = C_0 \, \Delta P \quad |\Delta P| < \mathrm{d}p_0, \tag{4}$$

where C_0 is a linearized flow coefficient, kg/s, Pa defined as

$$C_0 = C \, \mathrm{d}p_0^{n-1}, \tag{5}$$

where C is the flow coefficient, kg/s, Pa^n and n the flow exponent. The default limit value for linearization (dp_0) is 5 Pa in IDA-ICE 3.0, but this model was simulated using 0.1 Pa as the limit, because a slight tendency of the crack flow to be laminar below a pressure

Table 4
Wind pressure coefficients of a detached house

Wind angle (deg)	Wind pressure coefficients/facade											
	Sheltered				Rural				Exposed			
	F1	F2	F3	F4	F1	F2	F3	F4	F1	F2	F3	F4
0	0.06	−0.3	−0.3	−0.3	0.25	−0.6	−0.5	−0.6	0.5	−0.9	−0.7	−0.9
45	−0.12	0.15	−0.38	−0.32	0.06	0.2	−0.6	−0.5	0.25	0.2	−0.8	−0.6
90	−0.2	0.18	−0.2	−0.2	−0.35	0.4	−0.35	−0.3	−0.5	0.6	−0.5	−0.35
135	−0.38	0.15	−0.12	−0.32	−0.6	0.2	0.06	−0.5	−0.8	0.2	0.25	−0.6
180	−0.3	−0.3	0.06	−0.3	−0.5	−0.6	0.25	−0.6	−0.7	−0.9	0.5	−0.9
225	−0.38	−0.32	−0.12	0.15	−0.6	−0.5	0.06	0.2	−0.8	−0.6	0.25	0.2
270	−0.2	−0.2	−0.2	0.18	−0.35	−0.3	−0.35	0.4	−0.5	−0.35	−0.5	0.6
315	−0.12	−0.32	−0.38	0.15	0.06	−0.5	−0.6	0.2	0.25	−0.6	−0.8	0.2

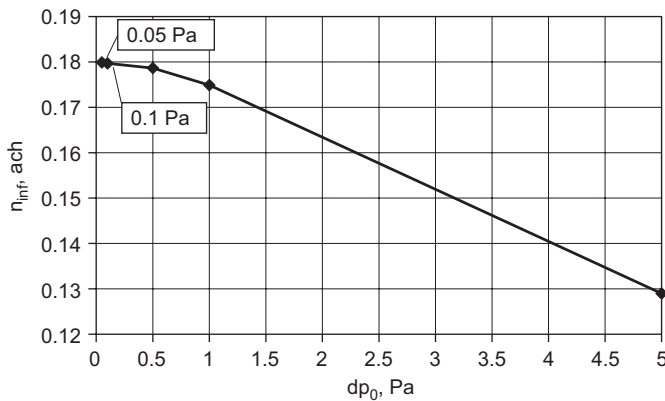The wind angle $0°$ corresponds to wind flowing from the south.

Fig. 4. Infiltration air change rate of the detached house simulated with the different limit value of linearization.

difference of 0.1 Pa was found [27]. In practice, the effect of linearization on mass flow is negligible with a 0.1 Pa limit, because the absolute pressure difference value over the envelope usually exceeds 0.1 Pa in these kinds of detached houses [28]. The infiltration air change rate of the modelling object is underestimated by about 30% if a 5 Pa limit for linearization is used (see Fig. 4), but the error caused by linearization is case dependent, because it depends on the pressure conditions and the value of the flow exponent.

In IDA-ICE 3.0, the IHR effect is not taken into account. However, in the current study, this effect is studied with the simplified model developed by Buchanan and Sherman [8]. In this model, the IHR effect is simulated, correcting the infiltration heat losses that are calculated in a conventional way ($q_{\text{inf}-c}$) [8] with an IHR factor ε, see Eq. (8), while the conduction heat losses are assumed to remain unchanged

$$q_{\text{inf}} = (1 - \varepsilon)q_{\text{inf}-c} \qquad (6)$$

The heat recovery factor ε is a function of the Peclet number (Pe), which is defined in this case as

$$Pe = \frac{Qc_{\text{p}}}{UA}, \qquad (7)$$

where Q is the infiltration mass flow, kg/s, c_{p} the specific heat of air, J/kg, K, U the thermal conductance, W/m², and K and A the surface area of building envelope, m². The heat recovery factor is defined as

$$\varepsilon = \frac{1}{Pe_{\text{inf}}} + \frac{1}{Pe_{\text{exf}}} - \frac{1}{e^{Pe_{\text{inf}}} - 1} - \frac{1}{e^{Pe_{\text{exf}}} - 1}, \qquad (8)$$

where Pe_{inf} is the effective Peclet number defined as the Peclet number divided by effective area ratio for infiltrating air f_{inf} and Pe_{exf} is defined for exfiltrating air in a similar way. The fractions f_{inf} and f_{exf} are defined as the ratio of the building envelope that is actively participating in the heat transfer process between the building envelope and the air,

$$f_{\text{inf}} = \frac{U_{\text{inf}}A_{\text{inf}}}{UA}, \qquad (9)$$

$$f_{\text{exf}} = \frac{U_{\text{exf}}A_{\text{exf}}}{UA}, \qquad (10)$$

where A_{inf} and A_{exf} correspond to the area of the envelope that is affected by infiltration or exfiltration, m² and U_{inf} and U_{exf} are thermal conductances of these parts, W/m², K. The preceding areas are not the physical areas of the cracks, but the areas that undergo thermal changes due to infiltration or exfiltration. Because it is not possible to derive detailed information from the studied house about, for example, the length or characteristics of the cracks inside the walls, the preceding areas are roughly approximated with the two-phase thermography test described in [10]. According to the test, about 5% of the interior surface of the envelope undergoes thermal changes due to leakage air flows at −50 Pa pressure difference. This result indicates that infiltration air flows mainly through the cracks in the timber-framed house equipped with a plastic air–vapor barrier. It is obvious that the fraction of surface area is lower than 5% at the normal pressure conditions, but the test result was used in the study, because this paper was intended to study the maximum effect of IHR in the simulated house. Under normal pressure conditions and with the balanced ventilation system, the studied house is mostly negatively pressurized on the base floor and positively pressurized on the top floor [28]. Because of this, infiltrating air is assumed to enter the house on the base floor and exfiltrating air to leave the house on the top floor. In that case, the estimated areas A_{inf} and A_{exf} are 6.6 and 10.1 m². The thermal conductances of these parts are assumed to be equal to the average U-values of the base floor (U_{inf}) and the top floor (U_{exf}). These approximations are used in the calculation of the heat recovery factor of the modelling object.

2.4. Weather data

According to the updated Köpper–Geiger climate classification [29], Finland belongs to the cold climate zone (D), which is a dominant climate type in North America and Asia. According to the Finnish building code [2], Finland is divided into four climate zones (I–IV) for energy calculations of buildings, see Fig. 5.
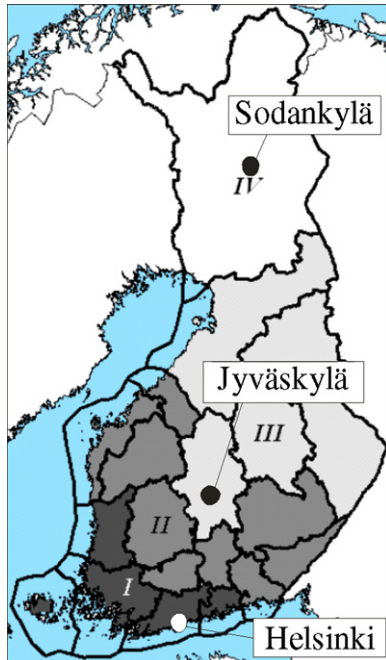
Fig. 5. The Finnish climate zones (I–IV) for energy calculations [2]. Simulations are carried out with hourly weather data of Helsinki, Jyväskylä, and Sodankylä.

Table 5
The average annual outdoor temperature T_{out} and wind velocity U_m at the weather stations in 1979 [32]

Location	Climate zone	T_{out} (°C)	U_m (m/s)
Helsinki (latitude 60°19′N, long 24°58′E)	I	4.3	4.1
Jokioinen (lat 60°49′N, long 23°30′E)	II	3.7	3.7
Jyväskylä (lat 62°24′N, long 25°41′E)	III	2.8	3.0
Sodankylä (lat 67°22′N, long 26°39′E)	IV	−0.8	3.2

The climate dependence of infiltration was studied simulating the modelling object with the hourly weather data of 1979 from Helsinki, Jyväskylä, and Sodankylä, see Table 5. According to Tammelin and Erkiö [30], these places represent the typical weather conditions of the climate zones. Climate zone II was not included in the study, because the conditions are quite similar to zone I (see Table 5). The weather data of 1979 are still commonly used as test-reference data for energy calculations, although outdoor temperatures have slightly increased because of global climate change. According to the weather statistics, the average outdoor temperature of a 10-year period has risen from the 1970s to the present by 1.1 °C in Helsinki, 1.3 °C in Jyväskylä and 1.4 °C in Sodankylä [31], showing that the outdoor air temperature difference between southern and the northern Finland has slightly decreased. Because of the temperature rise, heat energy use calculated with the old weather data is slightly overestimated.

3. Results

The results of the sensitivity analysis are presented and discussed below. The effect of various factors on infiltration and heat energy use of Finnish detached houses were simulated and a simple infiltration model based on the simulation results was derived. Results of the derived model and of several simplified models available from the literature were also compared against the results of IDA-ICE.

3.1. Studied cases

All the cases were simulated with three levels of airtightness. Almost completely airtight detached houses were described with a building leakage rate of $n_{50} = 0.15$ ach, while the airtightness of typical detached houses was simulated using $n_{50} = 3.9$ ach (see Table 1); the leakage air change rate $n_{50} = 10$ ach describes leaky detached houses. The studied factors of the sensitivity analysis, including 42 separate simulation cases, are listed in Table 6. The cases were simulated with sheltered, rural and exposed wind conditions (see Table 3). However, most of the cases were simulated with sheltered wind conditions because this type was considered to be the most common in Finland. This is because the Finnish detached houses are mostly located in population centers [33,34] with trees and other buildings in the vicinity. Additionally, Finland is mostly forested (78% of the total area) [35]. The effect of stack-induced infiltration alone is studied in the theoretical case of no wind effect. Most of the cases are also simulated using the leakage distribution (typical) that is based on the measurement result. The typical range of flow exponents of the studied Finnish buildings was included in the simulation study, but most of the cases were simulated with the mean value of 0.73.

3.2. Infiltration

Simulated annual average infiltration rate increases almost linearly as the building leakage rate increases, see Fig. 6. The infiltration is a climate-dependent phenomenon; the difference in infiltration rate between Helsinki (I) and Sodankylä (IV) is 10%, but it is only about 1% between Helsinki (I) and Jyväskylä (III), see Fig. 6(a). The resultant infiltration rate is almost the same in I and III zones, because the effect of lower outdoor air temperature in Jyväskylä is roughly compensated by weaker wind conditions, see Table 5. It is evident that the average infiltration rate of climate zone II is close to the results of zones I and III. This result indicates that Finland can be roughly divided into two parts based on the average infiltration rate of the detached houses: the combination of zones (I–III), where the infiltration is quite similar, and zone IV, where it is slightly increased. In the climate conditions of Helsinki, the effect of wind on the average infiltration rate of the studied house is less than 10% in the *sheltered* wind conditions, 35% in the *rural* and over 50% in the *exposed* wind conditions, see Fig. 6(b). This result indicates that, mostly in Finland, the stack-induced infiltration of the typical two-story detached house is more significant than wind-induced infiltration. But the wind conditions may increase the infiltration rate significantly, because the difference in infiltration rate between sheltered and exposed wind conditions is over 100% between the studied cases.

The maximum difference in the infiltration rate between the studied leakage distributions is about 50% in the sheltered wind conditions, see Fig. 6(c). The highest infiltration rate is caused by the *drafty roof/base floor* distribution (see Table 2) where the difference of height between the leakage openings is maximum. This leakage distribution causes an infiltration rate that is about 25% higher than the *typical* distribution, while the *drafty roof* and *drafty base floor* distributions cause an approximately 10–20% lower infiltration rate than the typical distribution. This result shows that distribution of the leakage openings has a significant effect on infiltration rate and it should be taken into account in the infiltration simulation.

The difference between the mechanical supply and extract air flow rates, which is the unbalanced part of the ventilation, flows through the cracks of the envelope in the form of infiltration and

Table 6
Studied factors of the sensitivity analysis

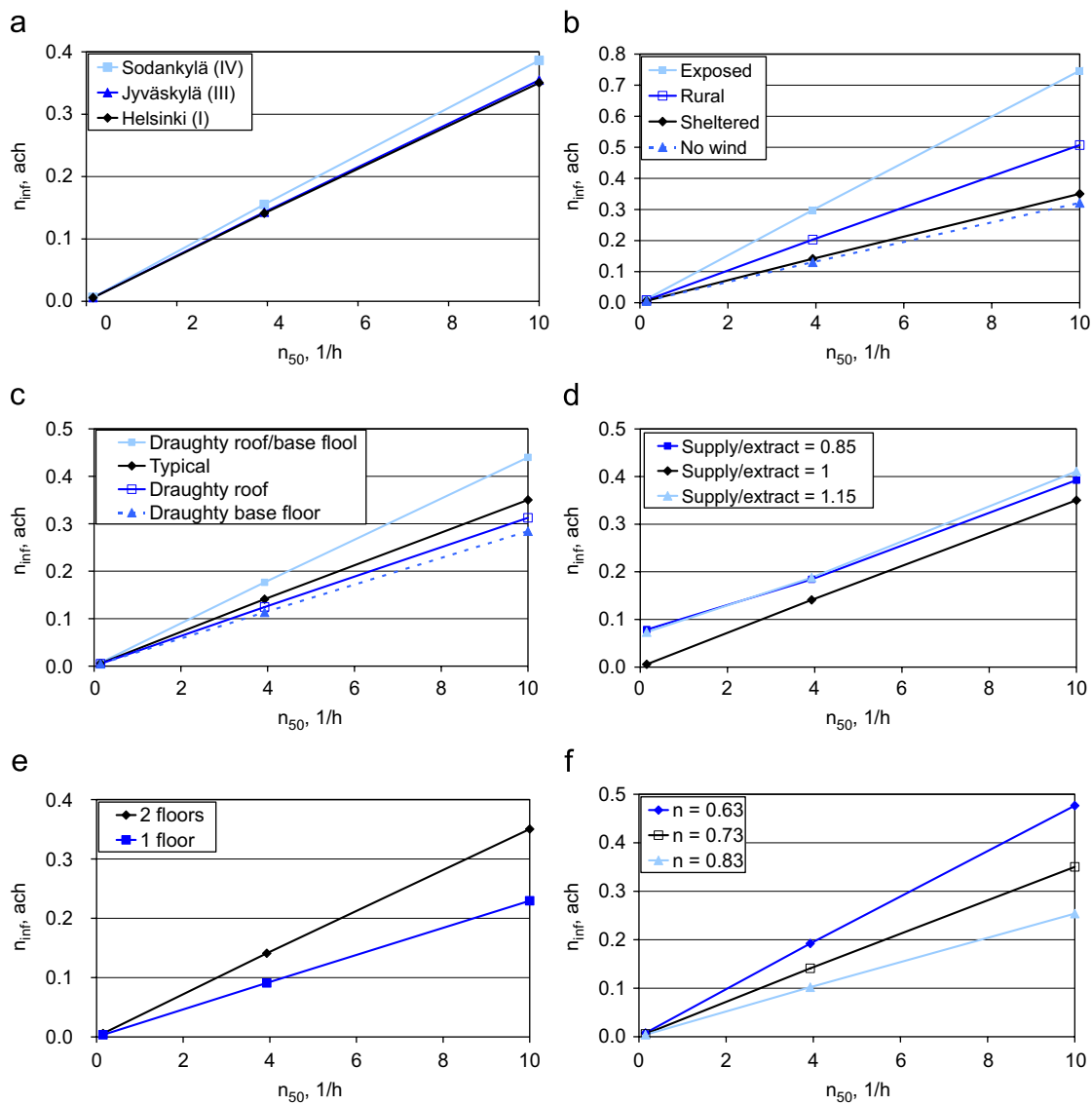| Climate	Wind conditions	Leakage distribution	Supply/extract	Height (floors)	Flow exponent	n_{50} (ach)
Helsinki	Sheltered	Typical	1	2	0.63–0.73–0.83	0.15–3.9–10
Jyväskylä	Sheltered	Typical	1	2	0.73	0.15–3.9–10
Sodankylä	Sheltered	Typical	1	2	0.73	0.15–3.9–10
Helsinki	Exposed	Typical	1	2	0.73	0.15–3.9–10
Helsinki	Rural	Typical	1	2	0.73	0.15–3.9–10
Helsinki	No wind	Typical	1	2	0.73	0.15–3.9–10
Helsinki	Sheltered	Dr. roof	1	2	0.73	0.15–3.9–10
Helsinki	Sheltered	Dr. base floor	1	2	0.73	0.15–3.9–10
Helsinki	Sheltered	Dr. roof/base floor	1	2	0.73	0.15–3.9–10
Helsinki	Sheltered	Typical	0.85	2	0.73	0.15–3.9–10
Helsinki	Sheltered	Typical	1.15	2	0.73	0.15–3.9–10
Helsinki	Sheltered	Typical	1	1	0.73	0.15–3.9–10

Fig. 6. The effect of several factors on the annual infiltration air change rate. Figures show the effect of the Finnish climate conditions (a), wind conditions of the building site (b), the leakage distribution (c), the balance of the ventilation system (d), the height of the building (e), and the flow exponent (f).

exfiltration. This is because intended air inlets or outlets do not exist in the envelope of the studied house. In this study, this unbalanced part is defined to belong to the infiltration flow rate and the calculation of the infiltration rate of the

negatively pressurized house (supply/extract = 0.85) is based on all the air that enters into the house through the envelope. Respectively, the infiltration rate of the positively pressurized house (supply/extract = 1.15) is calculated using outflow through

the envelope corresponding to the exfiltration rate of the house. The effect of the balance of the ventilation system on infiltration rate defined in this way is shown in Fig. 6(d). This figure shows that, if the building envelope is extremely airtight, infiltration air flow rate equals to the unbalance of the ventilation system. When the level of airtightness is normal or leaky, a 15% unbalance causes about a 10–30% increase in infiltration rate.

But, if the unbalanced part of the ventilation is not classified as part of the infiltration, unbalance in the ventilation system would decrease the infiltration rate.

The height of the building has a particular effect on the infiltration rate, see Fig. 6(e). When the height of the detached house is increased from one to two floors and air is able to flow freely between the floors, the average infiltration rate is increased about 60% on average. The infiltration rate is also increased by 36% when the flow exponent 0.73 is reduced by 0.1; it is decreased, respectively, by 27% if the flow exponent is increased by the same amount, see Fig. 6(f). This suggests that measured flow exponent should be used in detailed simulations of a single house. But, the average flow exponent 0.73 is appropriate to use for detached houses in Finland, when infiltration of housing stock is studied or measured value of the flow exponent is lacking.

The effect of internal flow resistances was also studied in the single case with the balanced ventilation system. According to the result, the different use of the internal doors has a slight effect on the infiltration rate. Compared with the normal use of the internal doors described in Chapter 2.2, the infiltration rate increase by 2% when all the internal doors were closed or decreased by 2% if all these doors were open. This result indicates that a slight pressure difference between the zones exist even if the air gaps of 20 mm below the doors were modelled.

According to the preceding simulation results, the average infiltration rate correlates almost linearly with the building leakage rate in most of the cases. Because of this, the average infiltration rate can be roughly approximated in most of the cases by the widely used relation dividing the building leakage rate n_{50} by a case-dependent denominator x,

$$n_{\mathrm{inf}} = \frac{n_{50}}{x}. \tag{11}$$

According to the simulation results, the denominator depends strongly on the case because the range of the x was from 12 to 44 in the studied cases. But, if this simple method is applied in cases where the building is extremely airtight and ventilation is not balanced, the denominator was 2. This simple approximation cannot be generalized to this kind of case, because the infiltration rate is mainly caused by the ventilation system, not by wind or stack effect. The effect of the studied factors on the denominator x can be simply taken into account using the numerical results shown in Fig. 6. Instead of deriving the average constant denominator for Finnish detached houses, the effect of the studied factors can be taken into account by using, for example, a simple adapted model expressing the denominator as a product of several correction factors, using the principle shown by Sherman [4],

$$n_{\mathrm{inf}} = \frac{n_{50}}{LWDHEB}, \tag{12}$$

where L is the climate-dependent factor, W the factor for the wind conditions, D the factor for leakage distribution, H the factor for height of the house, E the factor for the flow exponent, and B the factor for the balance of the mechanical supply and exhaust ventilation system. The values of the correction factors determined from the sensitivity analysis are listed in Table 7. The annual infiltration rate of Finnish detached houses can be roughly estimated substituting these correction factors into Eq. (12). According to this approach, the annual infiltration rate of a typical

Table 7
Correction factors for the adapted model

Climate zone	I–III	IV		
L	27	25		
Wind conditions	Exposed	Rural	Sheltered	
W	0.5	0.7	1	
Leakage distribution	Dr. roof/base floor	Typical	Dr. roof	Dr. base floor
D	0.8	1	1.1	1.2
Number of stories	1	2		
H	1.6	1		
Flow exponent	Larger cracks	Typical	Smaller cracks	
E	0.7	1	1.4	
Balance of ventilation	Balanced	Positively/negatively pressurized		
B	1	0.8		

one-story house with balanced ventilation system in sheltered wind conditions in the southern Finland is $n_{50}/43$ and the annual infiltration rate for a two-story house in similar conditions is $n_{50}/27$.

This simple model causes the error of -7% to 18% compared with the 40 simulation cases shown in Table 6; the average absolute value of error is 5%. Because the correction coefficients are based on the basic case (climate zone (I–III), sheltered wind conditions, typical leakage distribution, two-story building, typical flow exponent and balanced ventilation), the error grows when the adapted model is used in the other conditions. For example, the average error in 31 cases of sensitivity analysis with the flow exponent 0.73 is 4%, but the same error between the methods grows to 7% when the flow exponent is 0.63. The adapted model was also compared with the dynamic simulation in the five additional cases, where combination of the studied factors was changed. For example, a one-story house was simulated with the sheltered or exposed wind conditions in Helsinki or Sodankylä. The resultant average absolute value of error of these cases was 19%. Thus, the difference between the methods increases simply due to the different combination of the factors. It is evident that a discrepancy between the adapted model and the detailed dynamic simulation model would increase further, if the initial data (wind conditions, leakage distribution, balance of the ventilation, and flow exponent) of the case were much different from the factors shown in Table 6.

But the adapted model can be used in rough approximations when the detailed simulation is not possible to do. This adapted model can be used for houses where infiltration is predominately caused by wind and stack effect. It happens in the studied cases, for example, when the unbalanced part of the ventilation is in the range of $\pm 15\%$ and the level of airtightness is the normal or leaky, see Fig. 6(d). If the infiltration air flows are mainly caused by ventilation system, ventilation air flows should be taken into account in the model. Application of the adapted model indicates that the range of the denominator of Eq. (12) can range from 6 to 45 for two-story houses and from 9 to 73 for one-story houses, depending on the conditions.

The annual infiltration rate predicted by the adapted model, see Eq. (12), and a set of simplified models available in the literature are compared against the results of IDA-ICE, see Fig. 7. The studied simplified models are: the Kronvall–Persily model, the model developed by Sherman [4], the ASHRAE-model [36] and the simplified model of prEN ISO 13789 [37]. The Kronvall–Persily model and the model of Sherman are conversion formulas from pressurization test results (n_{50}) to average infiltration rate. The ASHRAE-model is a simplified version of LBL-infiltration model [25]. It is a single-zone model, which takes only wind and stack effect into account using the average wind velocity and indoor–outdoor air temperature difference of the studied period. Distribution of leakage openings is fixed in the ASHRAE-model, being quite evenly distributed over the envelope: walls (50%),
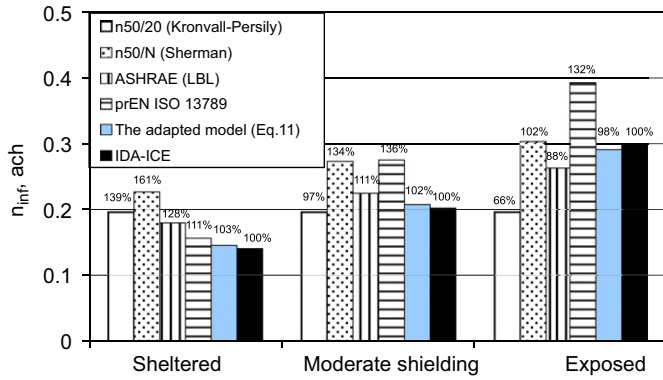
Fig. 7. The annual infiltration rate of a two-story detached house ($n_{50} = 3.9$ ach) calculated with different calculation methods.

Fig. 8. Infiltration air change of the detached house with three different building leakage rates in the sheltered wind conditions of Helsinki.

floor (25%) and ceiling (25%) [36]. The studied case is a two-story detached house in Helsinki with a balanced mechanical supply and exhaust ventilation system. The model of Sherman is developed for conditions of North America; the use of this model is questionable in the other conditions. However, this model was tested using the climate correction factor (18), corresponding roughly to the climate conditions of Helsinki according to the climate classification [29]. These models from the literature do not take the effect of mechanical ventilation system into account, expect for prEN ISO 13789, but the effect of the ventilation system is minor in the studied case because of the balanced system.

Compared with the simulation results, the simplified models mainly predict higher infiltration rates, especially in the sheltered and moderate wind conditions. The results of the simplified models vary from 34% lower to 61% higher infiltration rate, but the difference between the adapted model and IDA-ICE was only 2% or 3%. For all of the models from the literature, it was possible to predict the infiltration rate quite closely to the IDA-ICE rate, at least in one shielding class. But it is evident that the differences between the models vary in different wind conditions, because the shielding classes used by the models are not exactly similar. The correspondence between the IDA-ICE and Kronvall–Persily models was also good in moderate wind conditions.

If the average annual infiltration air change rate is used in the heat energy calculation, the outdoor air temperature dependence of infiltration air flows should be taken into account in the cold climate. During the heating season (normally from September to May in Helsinki), the infiltration air flow increases with the increasing temperature difference between indoor and outdoor air, see Fig. 8.

The fluctuation of the infiltration air change between the heating season and summer season can be taken into account by calculating the annual infiltration air change weighted by the temperature difference of the indoor and outdoor air

$$n_{\mathrm{inf}-e} = \frac{\sum\limits_{i=1}^{8760} (T_{\mathrm{in}} - T_{\mathrm{out}}^i)_i n_{\mathrm{inf}}^i}{\sum\limits_{i=1}^{8760} (T_{\mathrm{in}} - T_{\mathrm{out}}^i)_i}, \tag{13}$$

where $n_{\mathrm{inf}-e}$ is the average annual infiltration air change rate suitable for heat energy calculation, ach, n_{inf}^i is normal hourly infiltration air change rate, ach, T_{in} is a set point temperature of heating, °C, and T_{out}^i is hourly outdoor air temperature, °C. The weighted infiltration air change rate $n_{\mathrm{inf}-e}$ of the studied cases (see Table 6) was calculated with Eq. (13) using hourly infiltration rates simulated with IDA-ICE. This weighted annual infiltration rate was 3–20% higher that the original annual infiltration rate of the cases
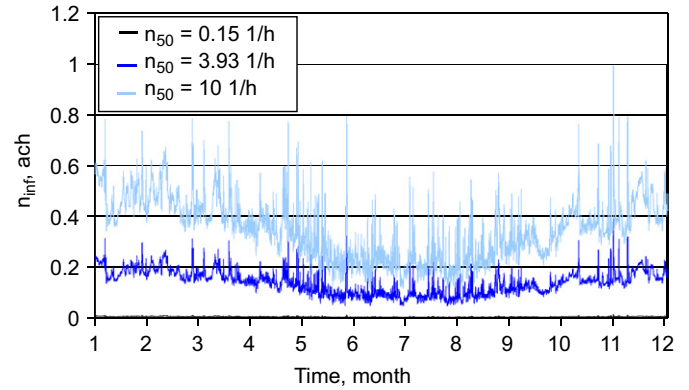
shown in Fig. 6, in which infiltration is mainly caused by wind and stack effect. Result of the adapted model can also be weighted analogously dividing the annual infiltration rate by a correction factor *e*. Based on the simulation results, the factor depends mainly on the wind conditions being 0.86 in the sheltered wind conditions, 0.93 in the rural or 0.97 in the exposed. A rough approximation of this correction factor can be considered to be 0.9 in the sheltered and moderate (rural) wind conditions, while the climate dependence of the factor is insignificant in Finland. Using the rough correction factor (0.9), previously defined approximations of annual infiltration rates of typical one- and two-story houses ($n_{50}/43$ and $n_{50}/27$) reduce to ($n_{50}/39$ and $n_{50}/24$).

3.3. Energy use

The performance of the IHR model was studied with several building leakage rates and effective areas of the envelope. According to the results, the IHR factor increases with the effective area and decreases with the building leakage rate, see Fig. 9. Fig. 9(a) shows that the IHR factor is at least 80% if the building leakage rate n_{50} is less than 10 ach and the whole envelope interacts with the air flow. However, the IHR factor decreases as the building leakage rate increases, because of the lower heat transfer between the walls and infiltrating air at higher air flow rates due to the shorter transit time of leaking air through the envelope. Assuming that the effective area (5%) of the modelling object does not depend on the building leakage rate, the IHR factor ranges from 10% to 94%, depending on the building leakage rate, see Fig. 9(b).

The effect of IHR is minor on energy use of the studied house because the effective area was considered to be only 5%. According to the studied cases, the IHR decreases the annual infiltration heat loss by 1–5 kWh/m^2 and the decrease in energy use of space heating including ventilation is from 1% to 4%, see Fig. 10(a). If the effective area was 20% of the envelope, this decrease would be 12%, or even 30% if the area corresponded to the whole envelope. But even if the heat recovery effect is small in the modelling object, it is taken into account in the following.

According to the simulation cases shown in Table 6, the annual energy use of space heating including ventilation ranges from 86 to 212 kWh/m^2 in the studied two-story house, depending mostly on climate and wind conditions. The total annual energy use of these cases is from 153 to 279 kWh/m^2, consisting of the heat demand of domestic hot water (25 kWh/m^2) and household- and HVAC-electricity (42 kWh/m^2). Heat energy use of the house is proportional to the infiltration rate, but the differences in heat energy use between the studied climate zones result mainly from
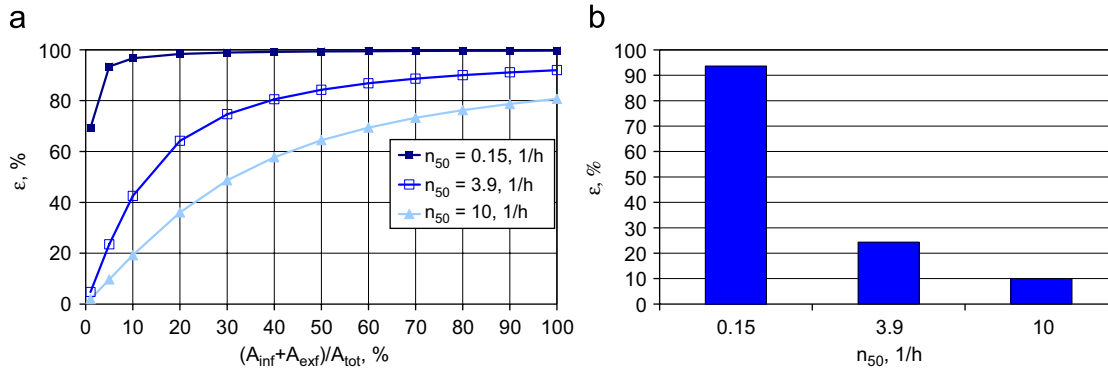
Fig. 9. Infiltration heat recovery factor of the detached house as a function of effective areas of the envelope (a) and building leakage rate (b).
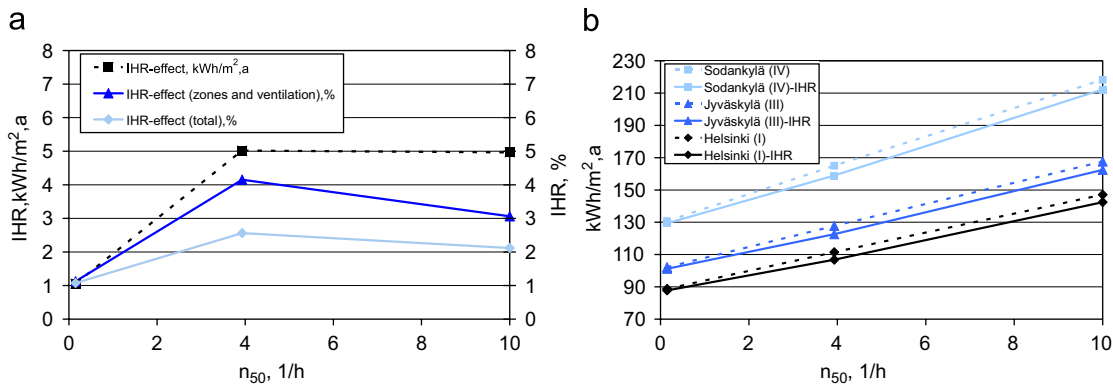

Fig. 10. The decrease in energy use because of the infiltration heat recovery effect (a) and energy use of the detached house in different climate zones, with and without infiltration heat recovery effect (b).

different conduction heat losses and heat energy use of an air handling unit, see Fig. 10(b). Compared with Helsinki (I), they are 13 kWh/m^2 higher in Jyväskylä (III) or 42 kWh/m^2 higher in Sodankylä (IV).

According to the studied cases, infiltration causes about 15–30% of the energy use of space heating including ventilation in the two-story detached house when the building leakage rate n_{50} is typical (3.9 ach), while the corresponding proportion is about 30–50% in the leaky house (10 ach). Because the correlation between the airtightness of the building envelope and the infiltration rate is almost linear, heat energy use of the houses also increases almost linearly at the same time. Therefore, the preceding correlation reduces into a simple rule of thumb: One unit change in n_{50} corresponds to a 7% change in the energy use of space heating including ventilation. At the same time, the change in total heat energy use is about 4%. In the studied cases, these increment percentages vary from 4% to 12% regarding space heating or from 2% to 7% regarding the total energy use. The variation of these percentages is mainly result from different wind conditions that were simulated, while the climate dependence of these percentages is minor.

4. Conclusions

According to the simulation results, the correlation between the airtightness of the building envelope and the annual infiltration rate is almost linear. Based on the average infiltration rate of detached houses, Finland can be roughly divided into two zones: the combination of climate zones (I–III), where the infiltration is quite similar, and zone IV, where it is slightly

increased. The stack-induced infiltration is typically dominant in the Finnish detached houses regardless of the climate zone.

The simple adapted model based on the simulation result can be used for rough approximation of the average infiltration rate of detached houses in Finland, while the other studied simplified models mainly predict higher infiltration rates than IDA-ICE, especially in sheltered and moderate wind conditions. The leakage distribution should be taken into account in the infiltration studies because it has a significant effect on the infiltration rate. The correction for the heat energy calculation in Finland can be performed normally by dividing the annual infiltration rate by the correction factor 0.9. The corrected approximations of annual infiltration rates of a typical one- and two-story house with a balanced ventilation system in sheltered wind conditions in Finnish climate zones (I–III) are $n_{50}/39$ and $n_{50}/24$, respectively.

Infiltration causes about 15–30% of the energy use of space heating including ventilation in a typical Finnish detached house. The resultant change in energy use of space heating is 7% on average, when the value of the building leakage rate n_{50} changes by one unit (1 ach). Respectively, the change in total heat energy use is about 4%. The IHR effect is minor in the typical Finnish detached house, but this effect can be increased with higher participation of the envelope, for example, by using dynamic insulation walls that are intentionally made porous.

References

[1] EN. Directive 2002/91/EC of the European Parliament and of the Council of 16 December 2002 on the energy performance of buildings. Official Journal of the European Communities, 4.1.2003, p. L1/65-71.

[2] D5 Finnish code of building regulations. Rakennuksen energiankulutuksen ja lämmitystehontarpeen laskenta [Calculation of energy consumption and heating power of buildings]. Ministry of the Environment. Guidelines; 2007 [in Finnish].

[3] Kronvall J. Testing of houses for air leakage using a pressure method. ASHRAE Transactions 1978;84(1):72–9.

[4] Sherman M. Estimation of infiltration from leakage and climate indicators. Energy and Buildings 1987;10(1):81–6.

[5] Dubrul C. Inhabitants behaviour with respect to ventilation. Technical note 23. UK: Air Infiltration and Ventilation Centre; 1988.

[6] Kohonen R, Kokko E, Ojanen T, Virtanen M. Thermal effects of air flow in building structures. Espoo, Finland: Technical Research Centre of Finland, Research Reports 367; 1985.

[7] Virtanen M. Thermal coupling of leakage air and heat flows in buildings and in building components. PhD thesis, Technical Research Centre of Finland, HVAC-Laboratory, Espoo, Finland, 1993.

[8] Buchanan C, Sherman M. A mathematical model for infiltration heat recovery. Lawrence Berkley Laboratory Report, LBL-44294, Berkley, USA, 2000.

[9] Qiu K, Haghighat F. Modeling the combined conduction—air infiltration through diffusive building envelope. Energy and Buildings 2007;39(11):1140–50.

[10] Jokisalo J, Kalamees T, Kurnitski J, Eskola L, Jokiranta K, Vinha J. A comparison of measured and simulated air pressure conditions of a detached house in a cold climate. Journal of Building Physics 2007; accepted for publication.

[11] Vinha J, Korpi M, Kalamees T, Eskola L, Palonen J, Kurnitski J, et al. Puurunkoisten pientalojen kosteus-ja lämpötilaolosuhteet, ilmanvaihto ja ilmatiiviys (Indoor temperature and humidity conditions, ventilation and airtightness of Finnish timber-framed detached houses). Research Report 131, Structural Engineering Laboratory, Tampere University of Technology, Tampere, Finland, 2005 [in Finnish].

[12] Korpi M, Vinha J, Kurmitski J. Massiivirakenteisten pientalojen ilmanpitävyys [Airtightness of the detached houses with massive structures]. Finnish Society of Indoor Air Quality (FiSIAQ), Helsinki University of Technology, HVAC-Laboratory, SIY Report 2007;25:247–52 [in Finnish].

[13] SFS-EN 13829. Thermal performance of buildings. Determination of air permeability of buildings. Fan Pressurization Method; 2001.

[14] ASHRAE. Handbook of fundamentals. US: American Society of Heating, Refrigerating and Air Conditioning Engineers; 1989.

[15] Orme M, Liddament M, Wilson A. Numerical data for air infiltration and natural ventilation calculations, Technical Note 44, Air Infiltration and Ventilation Centre, UK, 1998.

[16] Pientalobarometri. (Barometer of detached houses 2007). Pientaloteollisuusyhdistys r.y., Rakennustutkimus RTS. Oy, 2007 [in Finnish].

[17] Kalamees T, Kurnitski J, Korpi M, Vinha J. The distribution of the air leakage places and thermal bridges of different types of detached houses and apartment buildings. In: Proceedings of the second European Blower Door symposium, Kassel, Germany, March 16 and 17, 2007.

[18] C3 Finnish code of building regulations. Thermal insulation in a building. Helsinki, Finland: Ministry of the Environment. Regulations; 2003.

[19] Jokisalo J, Kurnitski J. Performance of EN ISO 13790 utilisation factor heat demand calculation method in a cold climate. Energy and Buildings 2007;39(2):236–47.

[20] D2 Finnish code of building regulations. Indoor climate and ventilation of buildings. Helsinki, Finland: Ministry of the Environment. Regulations and Guidelines; 2003.

[21] Shalin P. Modelling and simulation methods for modular continuous system in buildings. PhD thesis. Stockholm, Sweden: KTH; 1996.

[22] Moinard S, Guyon G, editors. Empirical validation of EDF ETNA and GENEC test-cell models. Subtask A.3, A Report of IEA Task 22, Building Energy Analysis Tools, 1999.

[23] Travesi J, Maxwell G, Klaassen C, Holtz M. Empirical validation of Iowa energy resource station building energy analysis simulation models, IEA Task 22, Subtask A, 2001.

[24] Achermann M, Zweifel G. RADTEST—Radiant heating and cooling test cases. Subtask C. A Report of IEA Task 22. Building Energy Analysis Tools, 2003.

[25] Sherman M, Grimsrud D. Infiltration–pressurization correlation: simplified physical modeling. ASHRAE Transactions 1980;86(2):778–807.

[26] Liddament M. Air infiltration calculation techniques—an application guide. UK: Air Infiltration and Ventilation Centre; 1986.

[27] Walker I, Wilson D, Sherman M. A comparison of the power law to quadratic formulations for air infiltration calculations. Energy and Buildings 1998;27(3):293–9.

[28] Kalamees T, Kurnitski J, Jokisalo J, Eskola L, Jokiranta K, Vinha J. Air pressure conditions in Finnish residences. In: Proceedings of the ninth REHVA World Congress-Clima 2007, Helsinki, Finland, 10.06.2007-14.06.2007.

[29] Peel M, Finlayson B, McMahon T. Updated world map of the Köpper–Geiger climate classification. Hydrology and Earth System Science Discussions 2007:439–72.

[30] Tammelin B, Erkiö E. Energialaskennan säätiedot—suomalainen testivuosi (Weather data for energy calculation—The Finnish test-year), Finnish Meteorological Institute, Weather Department—Technical Climatology, Report 7, Helsinki, Finlan, 1987 [in Finnish].

[31] Drebs A, Norlund A, Karlsson P, Helminen J, Rissanen P. Climatological statistics of Finland 1971–2000. Helsinki, Finland: Finnish Meteorological Institute; 2002.

[32] Meteorological Yearbook of Finland. Climatological data 1979, vol. 79(1a). Helsinki, Finland: The Finnish Meteorological Institute; 1980.

[33] Pientalobarometri (1999). (Barometer of detached houses 1999). Pientaloteollisuusyhdistys r.y., Rakennustutkimus RTS. Oy, 1999 [in Finnish].

[34] Statistics Finland. Official statistics on Finland, Statistics Finland, Press release 15.1.2008 (http://www.stat.fi/ajk/tiedotteet/v2008/tiedote_001_2008-01-15.html) [in Finnish].

[35] Sevola Y, editor. Forest Finland in brief. Helsinki, Finland: The Finnish Forest Research Institute; 2007.

[36] ASHRAE. Handbook of fundamentals, Chapter 26: ventilation and infiltration. US: American Society of Heating, Refrigeration and Air-Conditioning Engineers, Atlanta; 2001.

[37] prEN ISO 13789. Thermal performance of buildings, transmission and ventilation heat transfer coefficients, calculation methods; 2005.